

Prediction of critical load and critical crack length of a four-layered symmetric angle-ply laminate under Mode-II fracture

V.V. Venu Madhav¹, Ch. Praveen Kumar¹, V. Balakrishna Murthy^{1*} and AVSSKS Gupta²

¹Department of Mechanical Engineering, V. R. Siddhartha Engineering College,
Vijayawada-520007, India.

²Department of Mechanical Engineering, JNTU College of Engineering, Hyderabad, India

ABSTRACT

The main objective of the present work is to predict the critical crack length for a given load and critical load for a given crack length in case of an infinitely long four-layered angle-ply FRP laminates of symmetric ($\Theta/-\Theta/-\Theta/\Theta$) fibre orientation. The model is simply supported along two sides of infinitely long and subjected to a centre line loading parallel to supported edges. The crack is considered as a delamination at one end parallel to the supported edges in the mid plane of the laminate. The problem is modelled in commercial software ANSYS and the strain energy release rate (SERR) is calculated using Virtual Crack Closure Technique (VCCT). It is observed that the structure is subjected to mode-II fracture under the imposed loading and constraints. The effect of applied load and crack length on SERR is studied for different fiber angles of the laminate. Critical crack length and critical load are estimated from the interlaminar critical SERR.

Key words: Composites, FRP, Angle-ply, Strain energy release rate, VCCT, Delamination.

1. INTRODUCTION

The composite materials found several applications in various fields such as aeronautical, aerospace and automobile industries. Due to their excellent properties like strength to weight and stiffness to weight ratios, they substitute the traditional materials. The use of these composite materials has increased in the fabrication of structures. The common mode of failure observed in composite structures is interlaminar delamination. This may develop during manufacturing or during operational life of the laminate. Delamination may grow due to opening mode (mode I), shear modes (mode II and mode III) and mixed-mode (mode I + mode II). Interlaminar tensile stresses give rise to mode I fracture while interlaminar shear stresses result in mode II fractures. The spontaneous growth of a delamination while the applied load is constant is called "unstable growth". If the load has to be increased to promote further delamination, the growth is said to be "stable growth".

Interlaminar delamination results in the loss of stiffness and strength, which may lead to safety and reliability problems. Undetected subsurface delamination can lead to catastrophic failures without any external signs. The conventional design criteria are based on tensile strength, yield strength and buckling stress. These criteria are adequate for many engineering structures, but they are insufficient when the structures possess some cracks. Fracture mechanics compensates the inadequacies of conventional design concepts. Thus a better understanding of the fracture mechanics involved in interface delamination will enable to develop more effective damage tolerant and damage resistant structures.

The delamination growth behaviour of FRP composite laminates having two embedded delaminations at the interface under uniaxial and transverse loadings was studied by D. Chakraborty and B. Pradhan (2006). To calculate the internal stresses at the interface responsible for delamination, a three-dimensional FE analysis is performed. Effects of delamination size, shape and the centre distance between the two delaminations on individual strain energy release rate components were evaluated to assess the delamination behaviour. An experimental study was done by Pereira et al., (2004) on the mode II interlaminar fracture of carbon/epoxy multidirectional laminates. To define appropriate stacking sequences for end-notched flexure specimens, a three-dimensional FE analysis was first performed with starter delamination on $\theta/-\theta$ and $0^\circ/\theta$ interfaces. Pereira and Morais, (2004) conducted an experimental study on the Mode II interlaminar fracture of fabric glass/epoxy multidirectional laminates. By performing a preliminary finite element analysis, stacking sequences for end notched flexure specimens were chosen with starter delaminations on interfaces. It was found that with increasing in the ply angle ' θ ' for both $\theta/-\theta$ and $0^\circ/\theta$ specimens G_{IIC} values are increasing. Chengye et al., (2006) conducted a study to investigate the possibility of predicting delamination development in fibre-reinforced polymer specimens that have single off-axis insert layer and are subjected to 3-point bending. Finite Element method is used to facilitate the analysis of the energy release rate (G). Two analytical approaches are proposed to predict delamination size development in the beam test specimens. The prediction is then compared with experimental results. The delamination fracture of continuous carbon fibre/epoxy multidirectional-laminates under Mode I, Mode II and Mixed-Mode I/II loading conditions was characterized by Choi et al., (1999). The results revealed that the values for the interlaminar fracture energy at crack initiation for the $(-45^\circ/0^\circ/+45^\circ)_{2S}$ $(+45^\circ/0^\circ/-45^\circ)_{2S}$ multidirectional laminates were always significantly greater than that for the corresponding unidirectional (i.e., $0^\circ/0^\circ$) laminates. Young-Jin Yum and Hee You, (2001) performed mode I, mode II and mixed mode fracture tests to characterize the delamination of unidirectional graphite/epoxy composites. Double cantilever beam specimens are used for mode I test and end loaded split specimens are used for mode II test. The critical strain energy release rates were evaluated by beam theory and compliance method. Modified mixed mode bending tests were also performed to investigate the mixed mode I/II delamination. Jialai Wang and Pizhong Qiao (2003) evaluated the shear-mode (Mode II) fracture toughness of wood-wood and wood-fibre reinforced plastic (FRP) bonded interfaces using unique linear tapered end-notched flexure (TENF) specimens. Chakraborty and Pradhan (1999) examined the delamination initiation at the interface of broken and continuous plies in case of GR/E and GL/E laminates with broken central plies. A three-dimensional finite element analysis is performed with each layer of laminate which are modelled as homogenous and orthotropic. The effects of various factors such as ply thickness, fibre orientation and resin stiffness on G_c were studied for GR/E and GL/E laminates with broken central plies. Rebiere and Gamby (2008) proposed an energy criterion to study the damage evolution in a composite cross-ply laminate. This criterion is based on the computation of the partial strain energy release rate associated with each damage mechanism (transverse cracking, longitudinal cracking and delamination) and mode (I, II, III), which can predict and describe the initiation and propagation of the different damage mechanisms. The damage analysis using interlaminar fracture specimens was done by Allix

at al., (1995). Delamination specimens here are modelled as two beams connected by a damageable interface. Comparisons between numerical simulation and experiments have been performed for a wide class of specimens by means of FE analysis.

Srinivasa Rao et al. (2012) modelled four layered angle-ply laminates of symmetric and anti-symmetric nature having infinitely long along the supported edges. This paper dealt on fixation of finite element model length to simulate the infinite plate. They concluded that a length of 300mm is sufficient to model laminate of any fiber angle. The present analysis is an extension of the work of Srinivasa Rao (2012) for the prediction of critical load for a given crack length of 45mm and critical crack length for a given centre line load of 100 N/mm for different symmetric fibre angle orientations varying from 0° to 90° .

2. GEOMETRIC MODELLING

The geometric model considered for the present analysis has the dimensions of 100mm span, each layer of thickness 2.5mm($10/4=2.5$) and its length is infinite. The required length of FE model to represent an infinitely long angle-ply laminates is found to be 300 mm (Srinivasa Rao et al., 2012) from previous work. For predicting the critical load for a given crack length, an edge crack of 45mm length is taken at the centre interface of four-layered angle-ply FRP laminate. For predicting the critical crack length for a given load, the geometric model is subjected to a centre line loading of 100 N/mm.

2.1 FINITE ELEMENT MODELLING

Finite element mesh is generated using 8-node brick element SOLID 45 in ANSYS software which is shown in figure 1. This element is defined by 8 nodes having three degrees of freedom per node: translations in the nodal x, y and z directions. The element may have any spatial orientation. The element SOLID 45 has the capability to inherit orthotropic material properties and hence, best suited for analysing FRP composites.

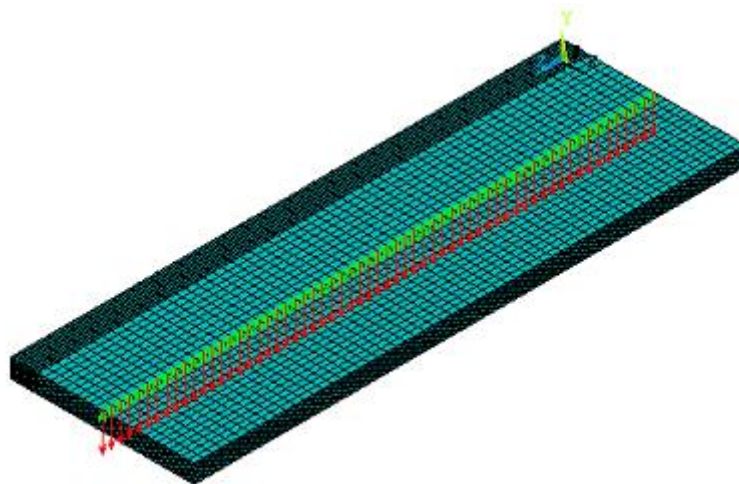


Figure 1: Finite element model with centre line loading

2.2 BOUNDARY AND LOADING CONDITIONS

The model is simply supported along the length of the laminate. A uniform centre line loading of 100 N/mm in downward direction is applied while determining the critical crack length for a given load. Figure 1 represents the model with a uniform centre line loading. Figure 2 shows the deformed model due to applied load.



Figure 2: Deformed model due to applied load

2.3 MATERIAL PROPERTIES

The following material properties of HTA/6376C carbon/epoxy prepreg composite are considered for the analysis (Nobert Blanco V., 2004).

- i) Young's Modulus, $E_1 = 120\text{GPa}$, $E_2 = 10.5\text{GPa}$, $E_3 = 10.5\text{GPa}$
- ii) Poisson's Ratio, $\nu_{12} = \nu_{13} = 0.3$, $\nu_{23} = 0.51$
- iii) Rigidity Modulus, $G_{12} = G_{13} = 5.25\text{GPa}$, $G_{23} = 3.48\text{GPa}$
- iv) Critical strain energy release rate under mode II fracture, $G_{IIC} = 1002 \text{ J/m}^2$

3. RESULTS AND DISCUSSION

The critical load for a given crack length of 45 mm is determined by varying the symmetric fibre angle orientations from 0° to 90° . From linear fracture mechanics, the strain energy release rates ' G_{II} ' is directly proportional to square of the load applied ' P^2 '. The advantage of this linearity is taken to extrapolate the strain energy values corresponding to different loads. The graphs are drawn between ' G_{II} ' and ' P^2 ' for different fibre angle orientations and the critical loads corresponding to $G_{IIC} = 1002 \text{ N/m}^2$ are determined. These are shown in figures from 3 to 9. The critical loads corresponding to each fibre angle are shown in the table 1 below. The decreasing of critical loads with increase in fibre angle is observed.

The critical crack length for a given load of 100 N/mm is determined by varying the symmetric fibre angle orientations from 0° to 90° . The graphs are drawn between ' G_{II} ' and ' a ' for different fibre angle orientations and the critical crack lengths corresponding to $G_{IIC} = 1002 \text{ N/m}^2$ are determined. These are shown in figures from 10 to 16. The critical crack lengths for fibre angles 0° , 15° and 30° are cannot be determined for the given load of 100 N/mm because the load applied is not adequate to produce the critical strain energy release rate (i.e., 1002 J/m^2). The critical crack lengths corresponding to each fibre angle are shown in the table 2 below. The critical crack lengths are decreasing with increase in fibre angle is observed.

$(\theta/-\theta/-\theta/\theta)$	Critical Load (N/mm) for a=45mm
0	176.7025
15	155.4704
30	120.9451
45	89.7772
60	67.1758
75	56.5428
90	54.8956

Table 1: Critical loads (N/mm) for a given crack length of a=45mm at different fibre angle orientations

$(\theta/-\theta/-\theta/\theta)$	Critical crack lengths (mm) for P=100 N/mm
0	–
15	–
30	–
45	38
60	31
75	27
90	26

Table 2: Critical crack lengths (mm) for a given load of P=100 N/mm at different fibre angle orientations

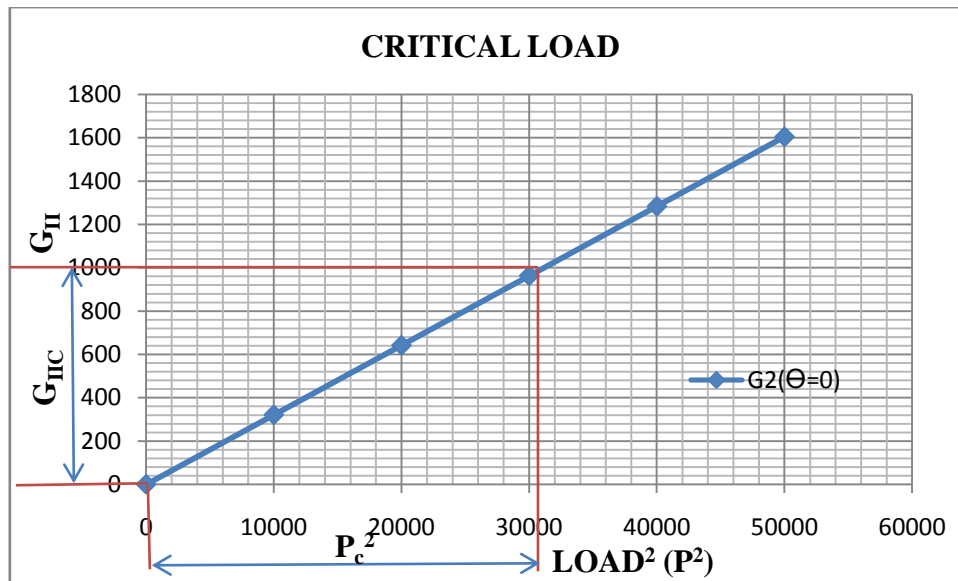


Figure 3: Variation of ' G_{II} ' in J/m^2 with respect to ' P^2 ' for a symmetric fibre angle orientation of 0^0

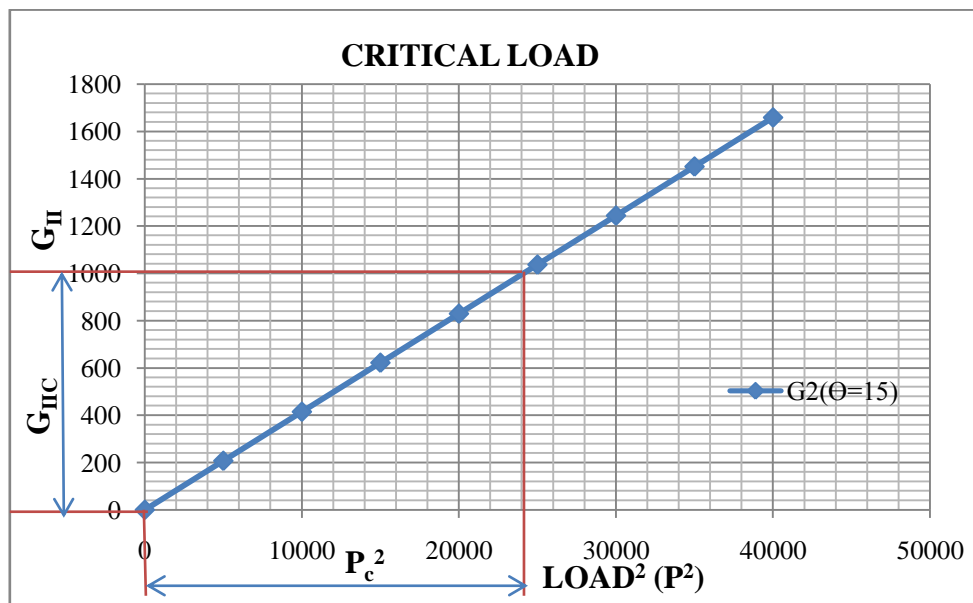


Figure 4: Variation of ' G_{II} ' in J/m^2 with respect to ' P^2 ' for a symmetric fibre angle orientation of 15^0

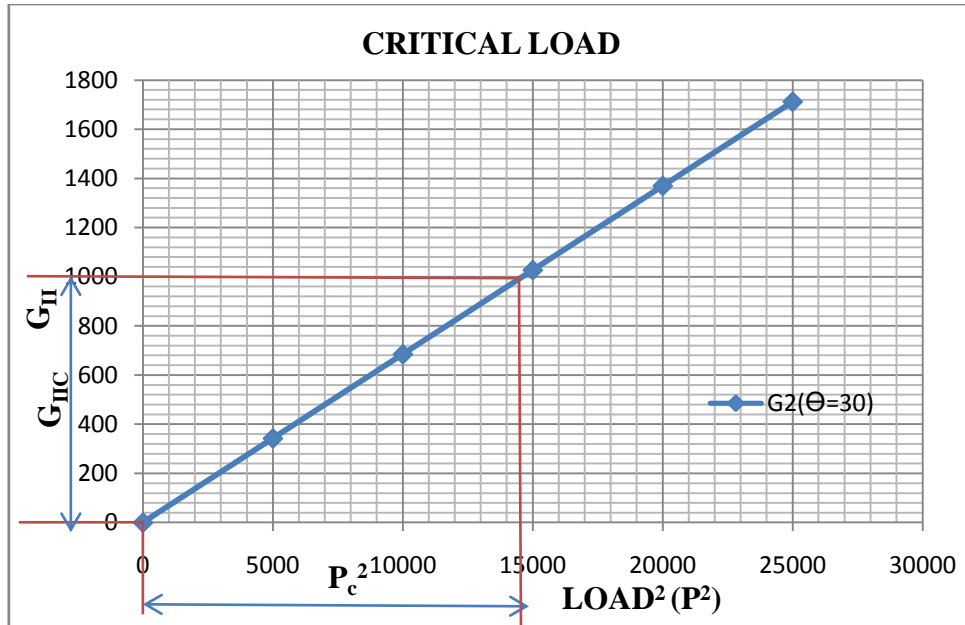


Figure 5: Variation of ' G_{II} ' in J/m^2 with respect to ' P^2 ' for a symmetric fibre angle orientation of 30^0

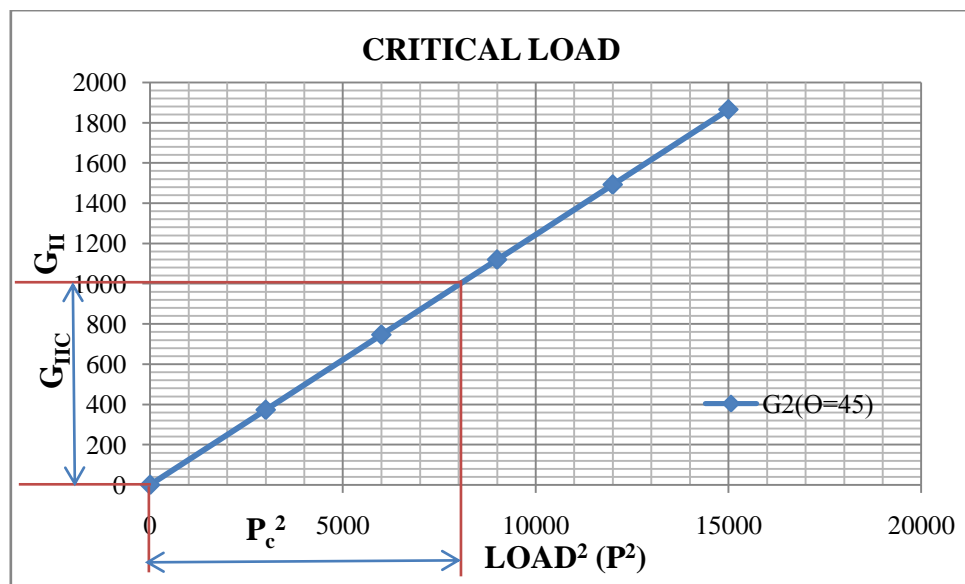


Figure 6: Variation of ' G_{II} ' in J/m^2 with respect to ' P^2 ' for a symmetric fibre angle orientation of 45^0

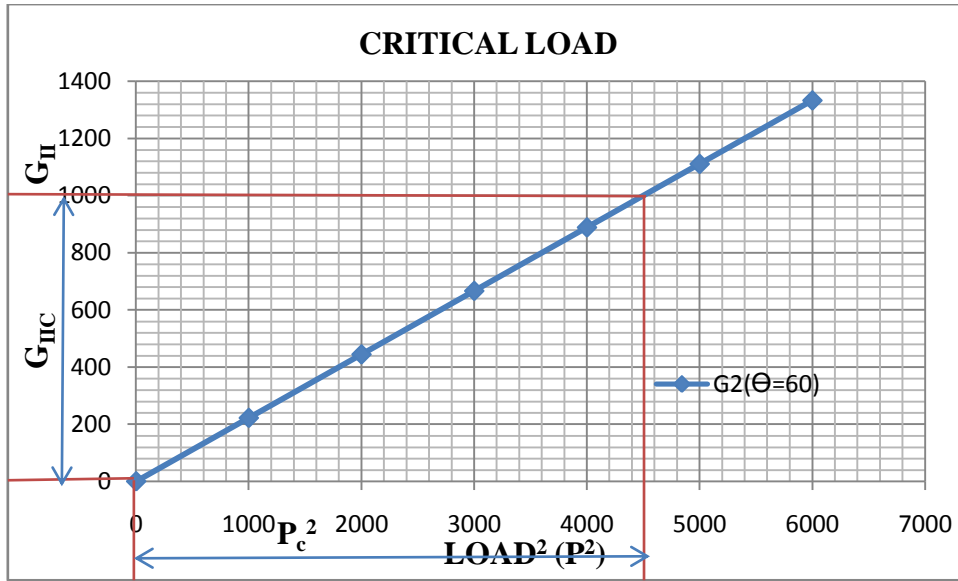


Figure 7: Variation of ‘ G_{II} ’ in J/m^2 with respect to ‘ P^2 ’ for a symmetric fibre angle orientation of 60^0

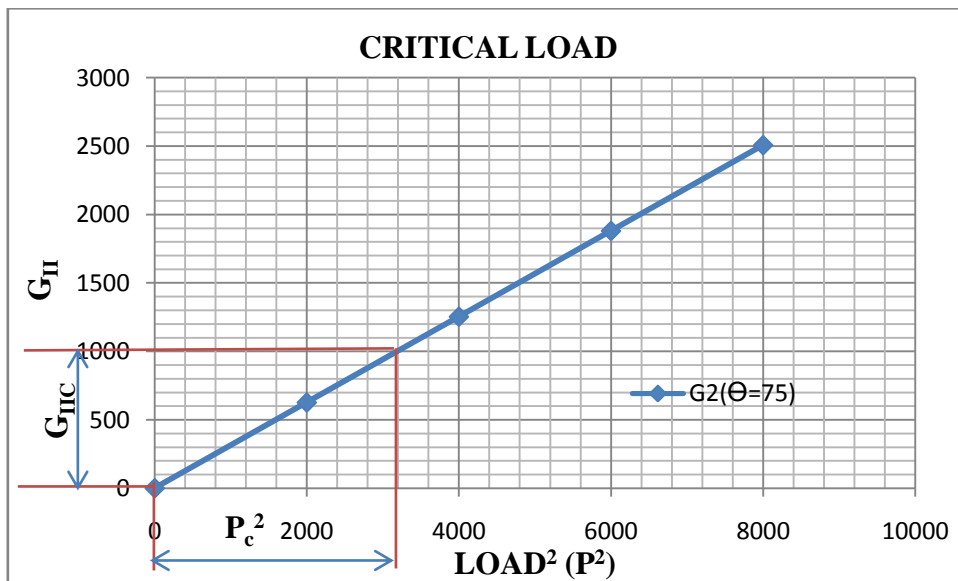


Figure 8: Variation of ‘ G_{II} ’ in J/m^2 with respect to ‘ P^2 ’ for a symmetric fibre angle orientation of 75^0

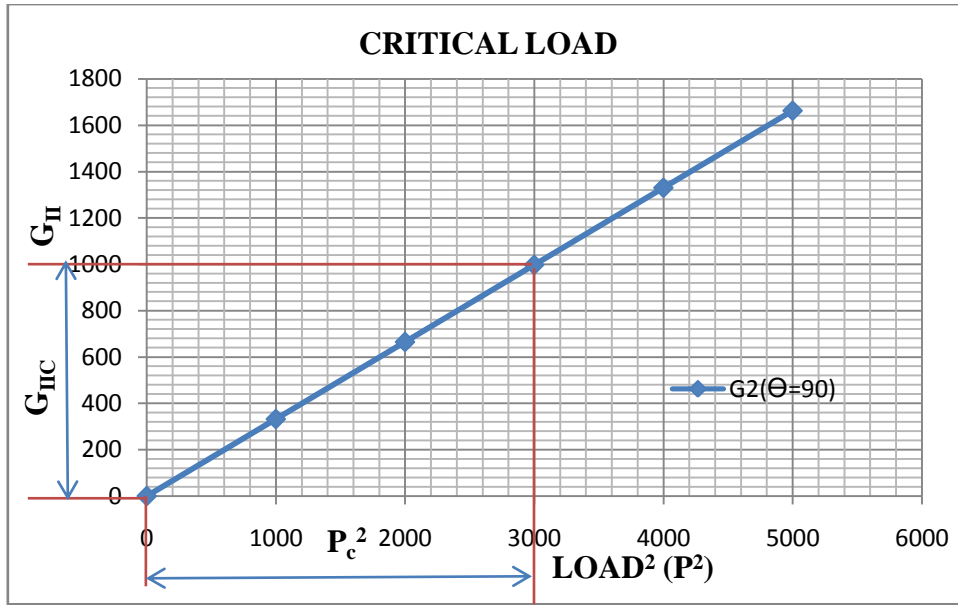


Figure 9: Variation of ‘G_{II}’ in J/m² with respect to ‘P²’ for a symmetric fibre angle orientation of 90⁰

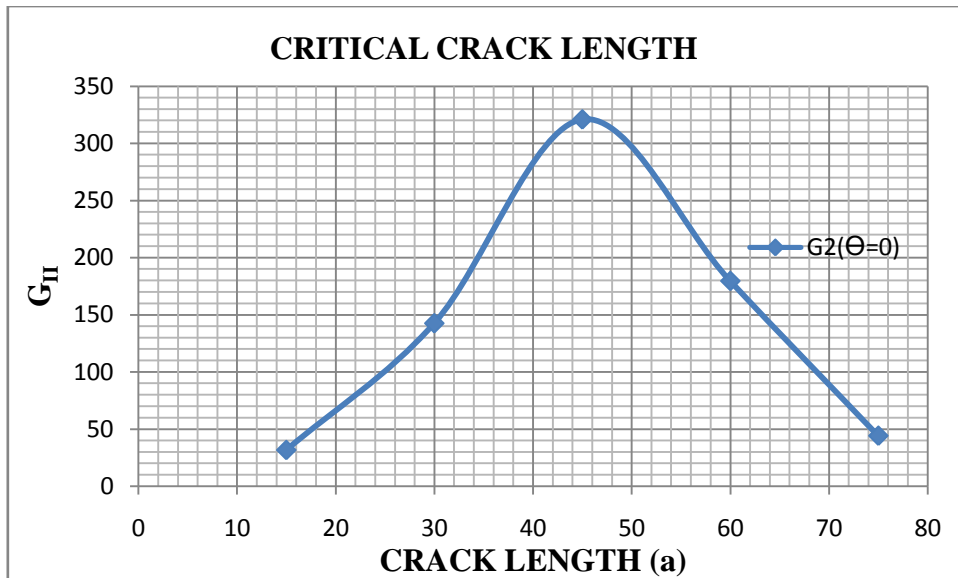


Figure 10: Variation of ‘G_{II}’ in J/m² with respect to ‘a’ for a symmetric fibre angle orientation of 0⁰

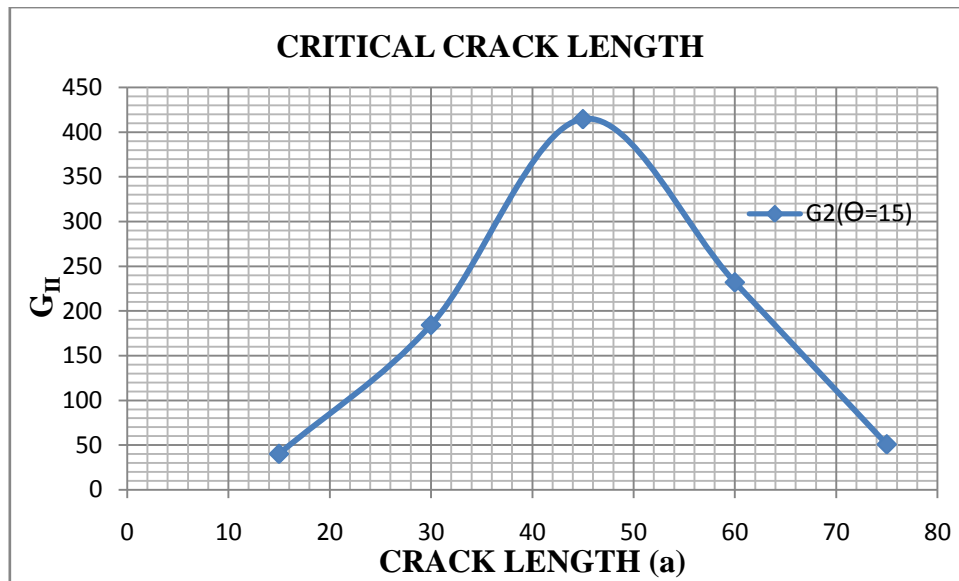


Figure 11: Variation of ' G_{II} ' in J/m^2 with respect to 'a' for a symmetric fibre angle orientation of 15^0

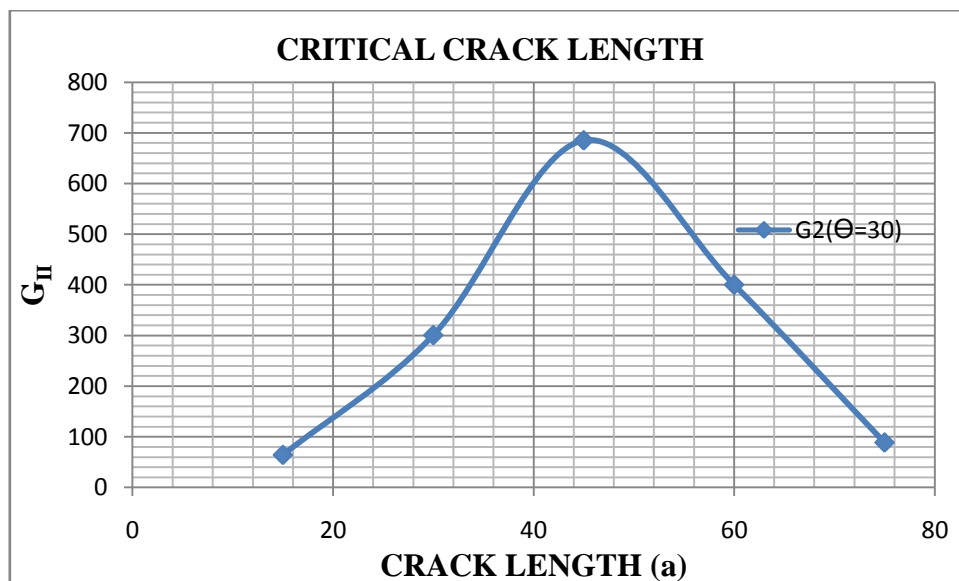


Figure 12: Variation of ' G_{II} ' in J/m^2 with respect to 'a' for a symmetric fibre angle orientation of 30^0

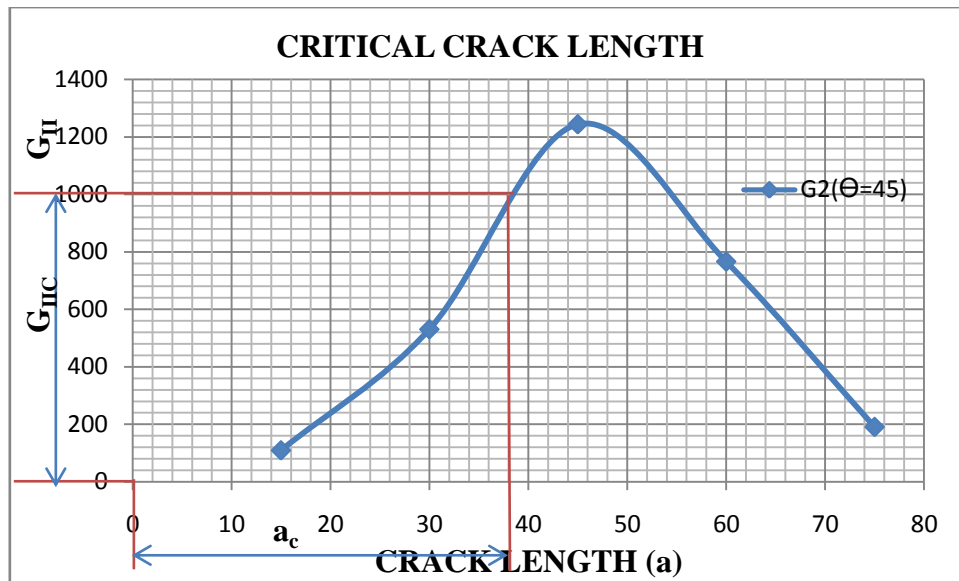


Figure 13: Variation of ' G_{II} ' in J/m^2 with respect to ' a ' for a symmetric fibre angle orientation of 45°

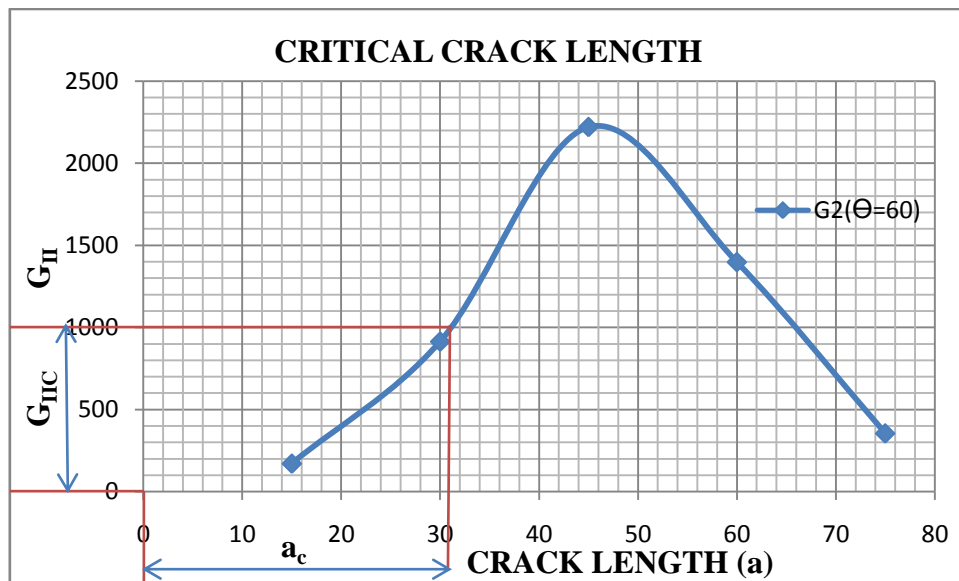


Figure 14: Variation of ' G_{II} ' in J/m^2 with respect to ' a ' for a symmetric fibre angle orientation of 60°

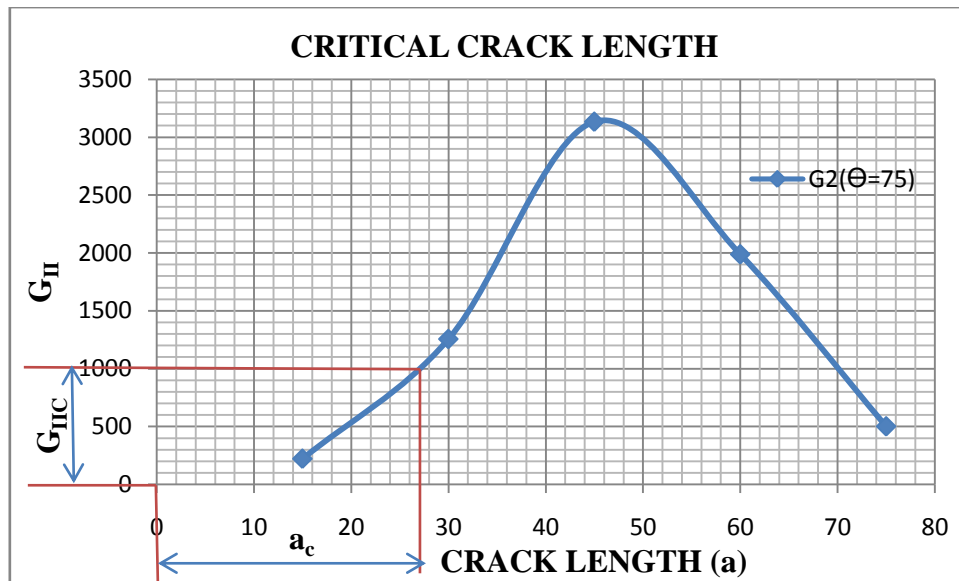


Figure 15: Variation of ' G_{II} ' in J/m^2 with respect to ' a ' for a symmetric fibre angle orientation of 75^0

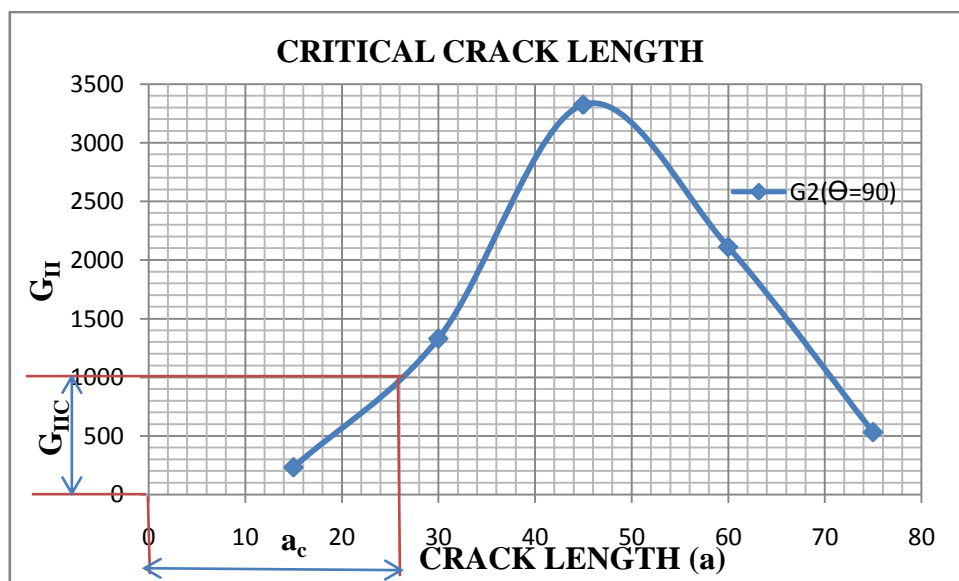


Figure 16: Variation of ' G_{II} ' in J/m^2 with respect to ' a ' for a symmetric fibre angle orientation of 90^0

4. CONCLUSIONS

The critical loads for a given crack length of 45mm and the critical crack lengths for a given load of 100 N/mm are determined for different fibre angle orientations from 0^0 to 90^0 . The following are observed.

- The critical loads are decreasing with the increase in fibre angle orientation

- The critical crack lengths are also decreasing with the increase in fibre angle orientation

5. REFERENCES

1. Allix, O.; Ladeveze, P.; Corigliano., (1995). Damage analysis of interlaminar fracture specimens. *Journal of Composite Structures.*, 31 (1), 61-74.
2. ANSYS reference manuals.
3. Chakraborty, D.; Pradhan, B., (2002). Fracture behaviour of FRP composite laminates with two interacting embedded delaminations at the interface. *Journal of reinforced plastics and composites.*, 21(8), 681-698.
4. Chakraborty, D.; Pradhan, B., (1999). Effect of ply thickness and fibre orientation on delamination initiation in broken ply composite laminates. *Journal of reinforced plastics and composites*, 18 (8), 735-758.
5. Chengye Fan.; Ben Jar, P. Y.; Roger Cheng, J. J., (2006). Energy based analysis of delamination in fibre-reinforced polymers under 3-point bending. *Journal of Composite Materials.*, 66 (13), 2143-2155.
6. Choi, N. S.; Kinloch, A. J.; Williams, J. G., (1999). Delamination fracture of multi-directional carbon/epoxy composites under mode I, mode II and mixed-mode loading. *Journal of composite materials*, 33, 73-100.
7. Jailai Wang.; Pizhong Qiao., (2003). Fracture toughness of wood-wood and wood-FRP bonded interfaces under mode II loading. *Journal of Composite Materials.*, 37(10), 875-897.
8. Nobert Blanco V., (2004). Variable mixed mode delamination in composite laminates under fatigue conditions: Testing and analysis. PhD thesis, Mechanical Engineering, Girona University.
9. Pereira, A. B.; de Morais, A. B.; Marques, A. T.; de Castro, P. T., (2004). Mode II interlaminar fracture of carbon/epoxy multidirectional laminates. *Journal of Composite Materials.*, 64(10-11), 1653-1659.
10. Pereira, A. B.; Morais, A. B., (2004). Mode II interlaminar fracture of glass/epoxy multidirectional laminates. *Journal on composites Part A: Applied Science and Manufacturing.*, 35 (2), 265-272.
11. Rebiere, J. L.; Gamby, D., (2008). A decomposition of the strain energy release rate associated with the initiation of transverse cracking, longitudinal cracking and delamination in cross-ply laminates. *Journal of composite structures.*, 84 (2), 186-197.
12. Srinivasa Rao B.; Praveen Kumar Ch.; Balakrishna Murthy V., (2012). Finite element modelling of infinitely wide angle-ply FRP laminates. *International Journal of Applied Science and Engineering, IPA*, Accepted for publication.
13. Young-Jin Yum.; Hee You., (2001). Pure mode I, II and mixed mode interlaminar fracture of graphite/epoxy composite materials. *Journal of reinforced plastics and composites.*, 20 (9), 794-908.